17th World Conference on Earthquake Engineering, 17WCEE

Sendai, Japan - September 13th to 18th 2020

TORSIONAL RESPONSES OF BUILDINGS CONSTRUCTED ON SOIL WITH INCLINED BEDROCK INFERRED FROM RECORDED MOTIONS

T. Takahira[(1)], Y. Tobita[(2)], X. Wang[(3)], R. Nishiura[(4)], M. Nagano[(5)]

[(1)] *Graduate Student, Tokyo University of Science, Chiba, Japan, 7115085@alumni.tus.ac.jp*
[(2)] *Structural Design Group, Asanuma Corporation, Tokyo, Japan, tobita-yoshinori@asanuma.co.jp*
[(3)] *Assistant Professor, Tokyo University of Science, Chiba, Japan, wangxin@rs.noda.tus.ac.jp*
[(4)] *Graduate Student, Tokyo University of Science, Chiba, Japan, 7114094@alumni.tus.ac.jp*
[(5)] *Professor, Tokyo University of Science, Chiba, Japan, nagano-m@rs.noda.tus.ac.jp*

Abstract

Generally, a combination of different foundations is used in buildings constructed on soil with inclined bedrock. In these cases, torsional response exerts force on the foundation during an earthquake. Tobita et al. (2018) investigated the torsional response of a seismically isolated building constructed on soil with inclined bedrock and equipped with a strong motion observation system. The strong motion records indicated that the torsional responses of the building were largely reduced by the isolated layer. Our study analyzes strong motion records with a focus on the amplification characteristics of soil with inclined bedrock and their effect on the torsional response of buildings with and without seismic isolation.

First, we analyzed the relationship between the predominant frequency and epicenter of strong motion records observed in a base-isolated building located on soil with inclined bedrock. The predominant frequencies of the recorded motions from three positions of the foundation in the building have obvious differences; these differences are due to the difference of layer thickness beneath each position. At the west end, where the bedrock depth is shallow, the nearer the epicenter is, the higher the predominant frequency.

Next, we conducted a seismic response analysis using a two-dimensional (2D) finite element method (FEM) for the soil and a three-dimensional (3D) moment-resisting frame model. To examine the feasibility of using a base-isolation layer to reduce the torsional response, we used a virtual model without a base-isolation layer.

Finally, we compared the torsional response characteristics of the models with and without base-isolation layers. In the former model, the ratio of the torsional response to the total horizontal response was much lower than that in the model without a base-isolation layer. Therefore, it can be said that an isolation layer contributes to a reduction in the torsional response of an upper structure.

Keywords: inclined bedrock, base-isolated building, torsional response, seismic response analysis

1. Introduction

In buildings constructed on soil with inclined bedrock, a combination of spread foundation and piles of different lengths are generally used for foundations. In these cases, torsional response along with translational response are exerted on the foundation during an earthquake because amplification factors and a time lag occur spatially because of varying layer thicknesses. Tobita et al. [1)] investigated the torsional response of a seismically isolated building constructed on soil with inclined bedrock and equipped with a strong motion observation system in the basement and on the first floor. The strong motion records indicated that the torsional responses of the building were largely reduced by the isolated layer. However, if this building is a conventional earthquake-resistant building without any base isolation, the response characteristics, including the torsional behavior of the entire upper structure during the earthquake, would be expected to change significantly. Therefore, it is important to compare the dynamic behaviors of base-isolated buildings and earthquake-resistant buildings. In this study, we first analyze the relationship between the predominant frequency and epicenter of the strong motion records observed in a base-isolated building located on soil with inclined bedrock. Next, we evaluate the ground motions of the inclined bedrock at multiple supporting points of the foundation using a two-dimensional (2D) FEM and seismic motions recorded at the center of the pit. To evaluate the structural responses, the evaluated ground motions are applied to the seismically isolated building as multiple input excitations. To examine the feasibility of using a base-isolation layer to reduce the torsional response, a virtual model for the conventional earthquake-resistant building is assumed to compare the seismic responses with those of the base-isolated building. Next, we compare the torsional response characteristics of the models with and without base-isolation layers. Lastly, we analyze in detail the responses of the model without a base-isolation layer.

2. The Building Used in This Study and its Subsurface Structure

The building scoped in this study is a six-story reinforced-concrete residential building located on soil with inclined bedrock, as illustrated in Fig. 1. Outlines of the target building are listed in Table 1. It is a seismically isolated building, in which seismic isolation devices (high damping laminated rubber) are placed between the first floor and the foundation. The longitudinal direction (East–West [EW]) is a moment-resisting frame structure, and the transverse direction (North–South [NS]) is a rigid frame structure with a shear wall. This building is equipped with six accelerometers: three on the upper surface of the foundation's bottom slab below the isolated layer and three on the lower surface of the first floor's slab just above the seismic isolation layer. They are arranged at the west end, at the center, and on the east end. The observation directions are two horizontal directions (NS and EW) and one vertical direction (UD) at the center, as well as one horizontal direction (NS) at both ends.

The subsurface structure beneath the building comprises two-layered soil consisting of a Dotan formation bedrock with Vs = 730 m/s and a silt-based alluvium surface soil with Vs = 140 m/s. The bedrock is inclined east and west on the site and has a height difference of approximately 23.5 m from the boring data. The azimuthal angle of the inclination of the bedrock is approximately 60° with respect to the building direction.

The foundation is supported by a cast-in-place concrete pile; the pile tips penetrate the bedrock. The pile lengths depend on the bedrock depth. At the northwest end, where the bedrock depth is the shallowest, a rubble trench foundation is used. The depth of the bedrock near the east end is GL-26 m, and the predominant period at the east end of the ground obtained from the H/V spectrum by the microtremor measurement is approximately 0.74 s.[1)]

3. Strong Motion Records

3.1 Relationships between the predominant frequency and epicenter distances

Observation records of 131 earthquakes in the building from 2000 to 2017 were obtained; the Mj and epicenter of each earthquake is indicated in Fig. 2. The 2011 Tohoku earthquake (Mw 9.0) was the largest among those recorded. The predominant frequency calculated from the Fourier amplitude spectra of the observed records (NS direction) obtained at the east and west ends of the base is traced in Fig. 3. At the west end, where the bedrock depth is shallow, in general, the lesser the epicenter distance, the higher the predominant frequency. By contrast, at the east end, where the bedrock depth is large, there is no difference in the predominant frequency approximately 1.35 Hz[1)] depending on the epicentral distance.

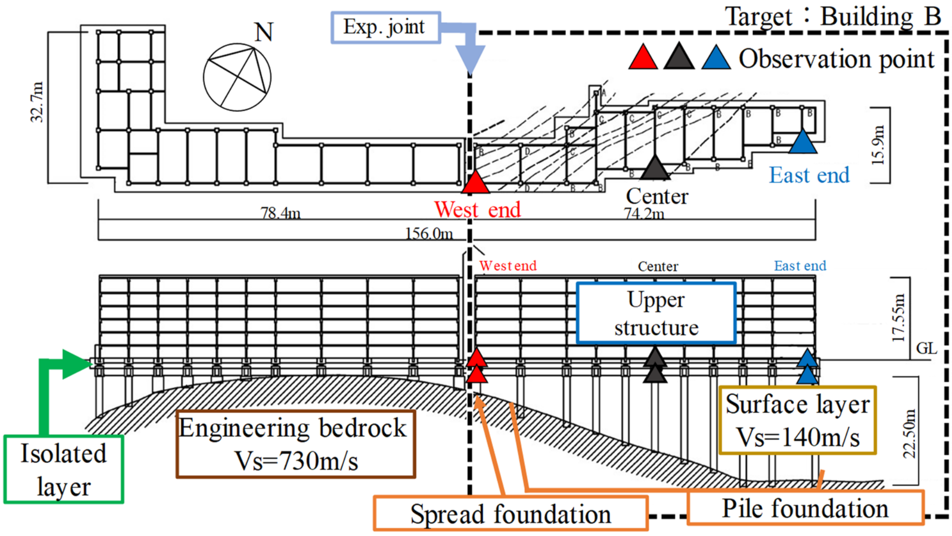

Fig. 1 Plan and cross-section schematics of the entire building; the area in the square with the dashed line (Building B) is the building used in this study

Table 1 Target building information

Location	Kanagawa prefecture		
Use	Residential building		
Construction area	958.6m^2	**Standard floor area**	692.6m^2
Number of floors	6 floors	**Height**	17.55m
Upper structure	Reinforced concrete (Basement: seismically isolated structure)		
	Longitudial direction: Rigid frame structure	Short-side direction: Rigid flame structure with a shear wall	
Foundational structure	Combination of a spread foundation and cast-in-place concrete piles		

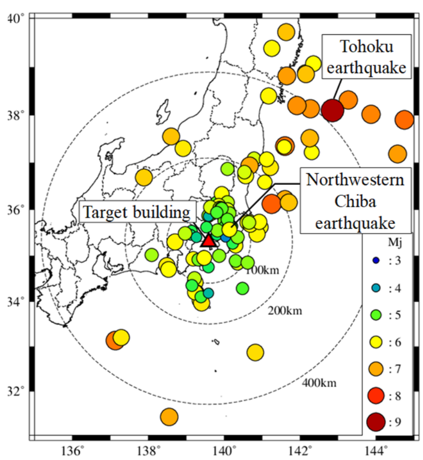

Fig. 2 Distribution of epicenters and the Mj of recorded strong motions

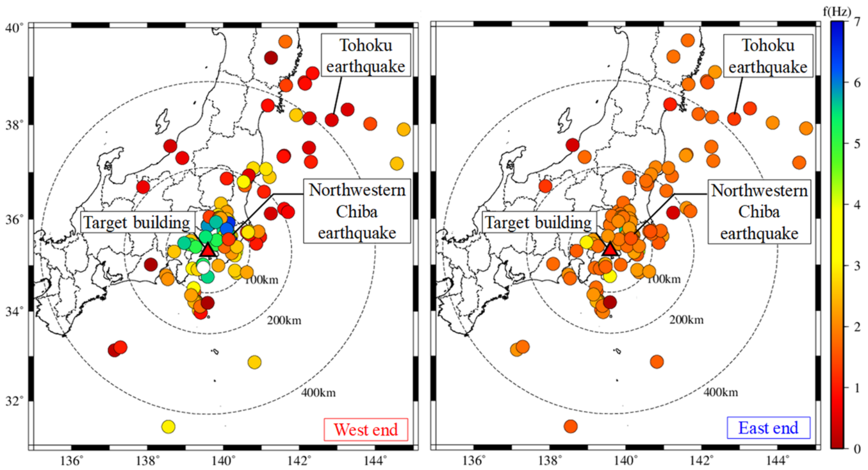

(a) (b)

Fig. 3 Distribution of predominant frequencies extracted from Fourier amplitude spectra of the strong motions of the bases at the (a) west end and (b) east end of the building

3.2 Earthquake records for seismic response analysis

Table 2 presents the seismic response analysis that was performed for two earthquakes in this study; the two earthquakes are the Tohoku earthquake, which occurred on March 11, 2011 and is the largest acceleration in the observation records at the west end of the foundation, and the Northwestern Chiba earthquake, which occurred on July 23, 2005 and is the second largest acceleration in the observation records at the west end of the foundation. The observed waveforms and pseudo-velocity response spectra at the base of both earthquakes are plotted in Fig. 4. Both earthquakes induced torsional vibration at the foundation.[1)3)]

Table 2 Target earthquake information

Date Time	Mw	Epicenter	Distance
2005 Northwestern Chiba earthquake			
2005/07/23 16:35:06	5.9	Northwestern of Chiba Pref.	66km
2011 Tohoku earthquake			
2011/3/11 14:47:47	9.0	Sanriku offshore	438km

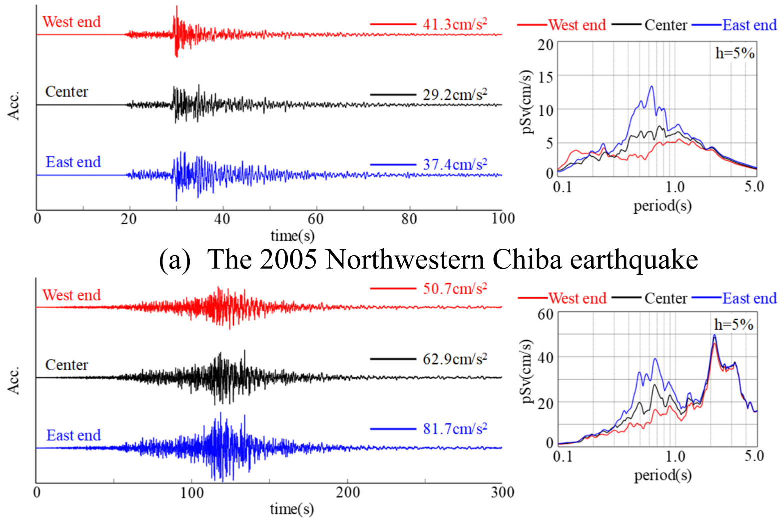

(a) The 2005 Northwestern Chiba earthquake

(b) The 2011 Tohoku earthquake

Fig. 4 Observed records at basement level (NS direction)

4. Construction of the Analysis Model

4.1 Subsurface structure

If the subsurface structure is rotated 60° counterclockwise from the building direction, it can be regarded as 2D-layered soil with bedrock inclination. This ground was modeled by 2D FEM, and the 2D soil responses to the vertical incidences of out-of-plane (SH) and in-plane (SV) waves were evaluated by a frequency response analysis. This model reproduced the observation records well[3)5)] and made it possible to calculate the ground motion at each base position of the building model. See the references[3)5)] for details of the model's analysis and simulation.

4.2 Upper structure

In this study, we employed a three-dimensional (3D) moment-resisting frame model for the step-by-step seismic response analysis of the buildings. SNAP version 7 from Structural Systems Co. was used for calculation. We built a model composed of the upper structure and seismically isolated layer (hereinafter referred to as the "base-isolated model") and a model that fixes the first floor and does not consider the seismic isolator (hereinafter referred to as the "earthquake-resistant model"). The upper structure was modeled with columns, beams, panels, floor members, and seismic walls, as seen in the overhead view in Fig. 5. All structural members were assumed to be elastic, and each layer had a rigid floor. The restoring force characteristics in the horizontal direction of the seismic isolation device were evaluated with an MSS model consisting of 12 springs with non-linearity, as will be stated in the next section. The vertical stiffness was evaluated by a single-axis spring model and was assumed to be elastic. The earthquake-resistant model was used under the assumption that the interaction with the soil was ignorable; ground motions evaluated at the isolator's positions were input directly to the base. Damping for the upper structure is proportional to the initial stiffness, and $h = 0.02$ with respect to the first natural period when the first floor is fixed. The internal viscous damping of the seismic isolation device is $h = 0.01$ with respect to the first natural period when the seismic isolation layer is 10% deformed.

4.3 Evaluation of stiffness of seismic isolation devices

Generally, the design-based formula for the stiffness of a seismic isolation device is determined for a shear strain of 10% or more. For small earthquakes with a shear strain of less than 10%, the stiffness of the design-based formula underestimates the actual stiffness. According to Morii et al.[4)], the equivalent stiffness K_{eq} at the time of a small deformation of a highly damped laminated rubber is expressed by Eq. (1):

$$K_{eq} = \frac{a \cdot K_{eq,\gamma=100\%}}{(1+\gamma/\gamma_r)} \tag{1}$$

$K_{eq,\ \gamma=100\%}$ is the equivalent stiffness at 100% shear strain, γ is the shear strain, and γ_r is the reference strain. Tobita et al.[5)] calculated the coefficients of Eq. (1) as α = 14 and $\gamma_{0.5}$ = 3.0% from the observation records at the center of the building and used these as the equivalent stiffness amounts of the seismic isolation devices. The design-based formula in Fig. 6 underestimates the stiffness in Eq. (1) for a shear strain of less than 10%. The restoring force characteristics of the seismic isolation devices are standard trilinear characteristics that approximate the stiffness for each strain from the Eq. (1) for the Northwestern Chiba earthquake, which had a shear strain of less than 10%. For the Tohoku earthquake, which exceeded a 10% shear strain, we used the

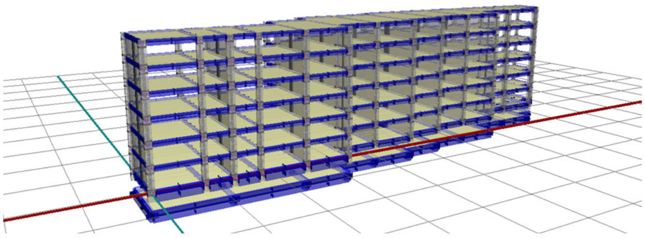

Fig. 5 3D frame model of the buiding

Table 3 Natural periods of analysis models

	Base-isolated model		Earthquake-resistant model
	Design eq.	Eq. (1)	
Stiffness of isolators	10%	5%	
EW	1.691s	1.342s	0.514s
NS	1.640s	1.274s	0.181s
Torsional	1.520s	1.187s	0.224s

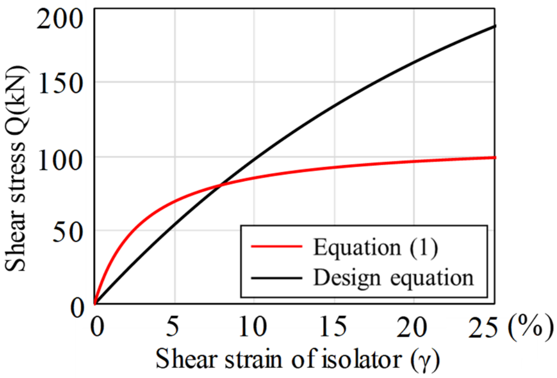

Fig. 6 Restoring force characteristics of isolation devices

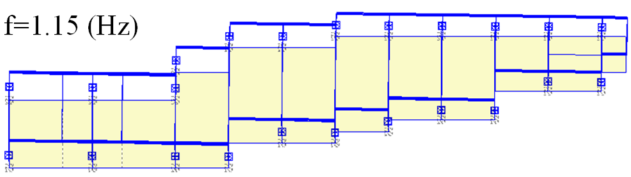

Fig. 7 Maximum displacements of the first mode of the base-isolated model (Eq. [1], γ = 0)

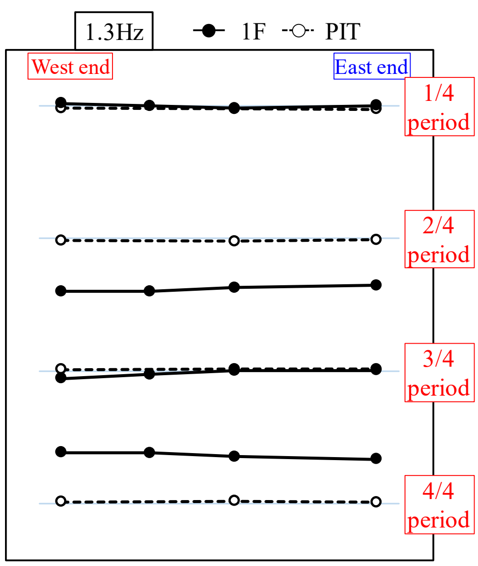

Fig. 8 Displacement of the first mode extracted from the micrometer measurement

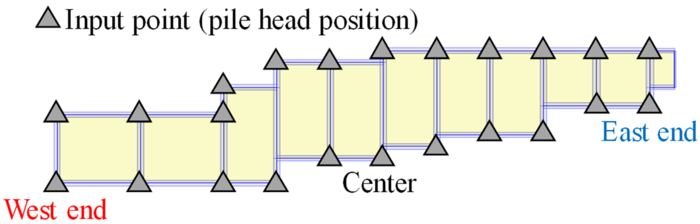

Fig. 9 Input points at the base are depicted by triangles

strain-dependent bilinear model defined in the design-based formula. Table 3 presents the results of the eigenvalue analysis. Nishiura et al. reported that there was a translational vibration in the NS direction at 1.3 Hz on the first floor according to the results of the microtremor measurements of the building.[6) 7)] The primary eigenmode in the NS direction at the initial stiffness of the seismic isolation device in the base-isolation model using Eq. (1) is traced in Fig. 7. The vibration mode obtained from the microtremor measurement is traced in Fig. 8. The lateral mode in the NS direction from the eigen analysis was 1.15 Hz, which is almost consistent with the results of the microtremor measurement.

4.5 The simulated results of the base-isolated model

For the pile position of the building model foundation in Fig. 9, the responses on the ground surface were calculated by 2D FEM, and these were used as input motions to the upper structure. The input directions had two horizontal components (NS and EW). In Fig. 10, accelerograms and their response spectra were evaluated by model analysis at 1F of the base-isolated model; these results were compared with the observation records of the two earthquakes. Although the rigidity of the seismic isolation devices at the time of the small deformation was underestimated in the later phase when the amplitude was small during the Tohoku earthquake; the simulated results in both earthquakes generally reproduced the observation records well.

5. Responses of the Base-Isolated Model, Focusing on Reduction of Torsional Motion

Seismic response analyses were performed using the records of the 2005 Northwestern Chiba earthquake and the 2011 Tohoku earthquake to investigate the responses of the base-isolated model; the focus was on the reduction of torsional motion in comparison with the earthquake-resistant model.

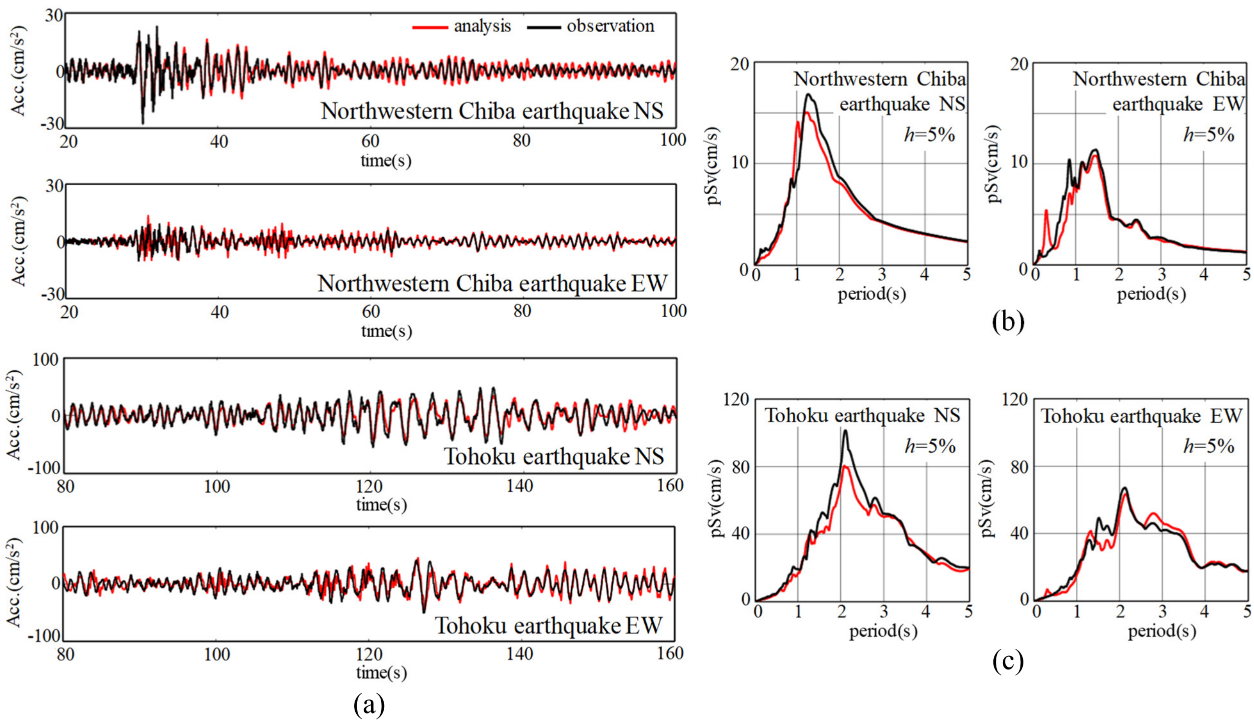

Fig. 10 Comparison between (a) calculated acceleration response waveforms and records at 1F. pSv of (b) Northwestern Chiba Earthquake, and (c) Tohoku Earthquake

5.1 Maximum responses

The maximum inter-story drift angle at the center of gravity of each floor of the two models is traced in Fig. 11. In both models, the inter-story drift angle in the NS direction was much smaller than that in the EW direction; this is due to the existence of the seismic walls. The inter-story drift angle of the upper structure was greatly reduced by the seismically isolated layer, compared with the earthquake-resistant model for the Northwestern Chiba earthquake. For the Tohoku earthquake, the effect of the isolators was more pronounced in the EW direction.

The maximum absolute acceleration values at three points, the west end, the center, and the east end, are traced in Fig. 12. Compared with that of the earthquake-resistant model, the maximum acceleration of the upper structure and the maximum inter-story drift angle of the base-isolated model were reduced in both earthquakes. When we compared three points in the NS direction of both earthquakes in the base-isolated model, the maximum acceleration increased toward the east, and the same tendency as the first floor[1)] could be seen uniformly throughout the upper structure. Since the torsional response of the input ground motion is small in the EW direction, the maximum acceleration of the upper structure in the base-isolated model is almost uniform at the three points.

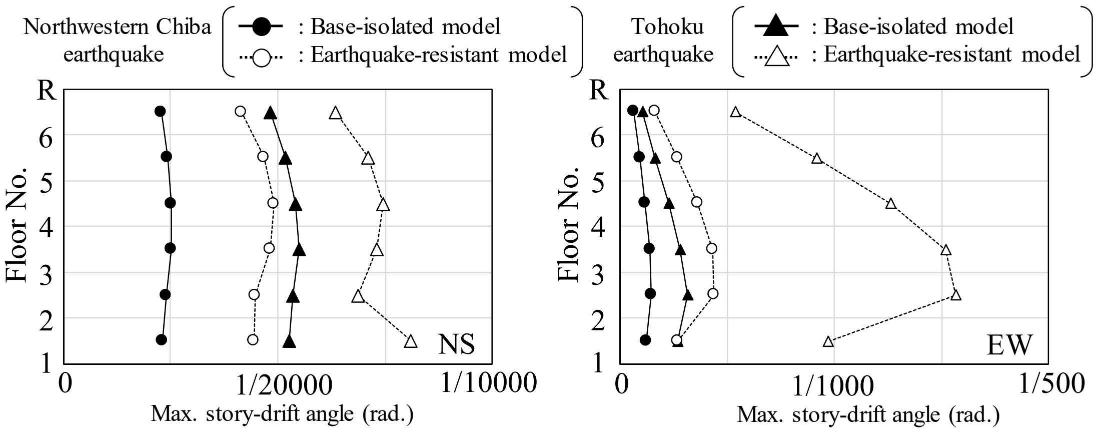

Fig. 11 Maximum story-drift angles at the center of gravity of each floor

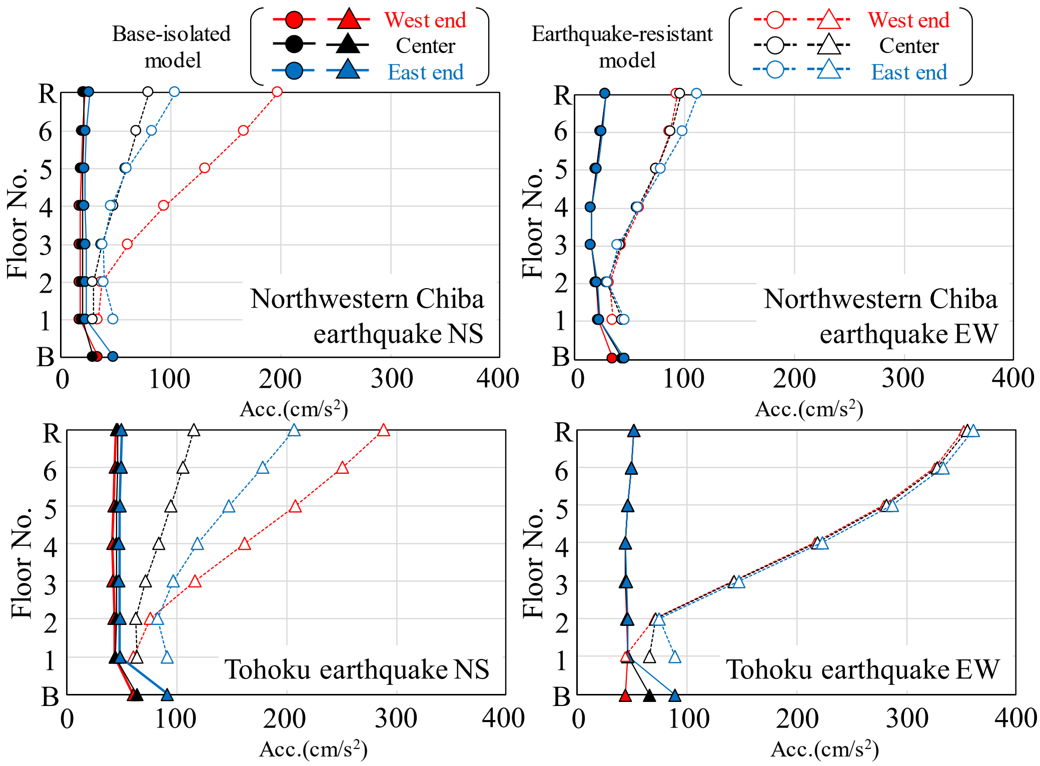

Fig. 12 Analysis results of the maximum acceleration at each floor during the Northwestern Chiba earthquake and the Tohoku earthquake

5.2 Comparison of torsional responses

The planar distribution of the inter-story drift of the sixth story is traced in Fig. 13. In the base-isolated model, the inter-story drift slightly and linearly increases toward the east side of the building. By contrast, in the earthquake-resistant model, the inter-story drift is bow-shaped and large at both ends, approximately 2–3 times that of the center. Fig. 13 also illustrates the results, in which the seismic wave at the west end of the ground is applied to all pile head positions, ignoring the spatial variation of ground motions that are due to the bedrock slope. Since the input seismic motion has no torsional component in this case, the torsional response of the building is small, and the inter-story drift has a linear distribution.

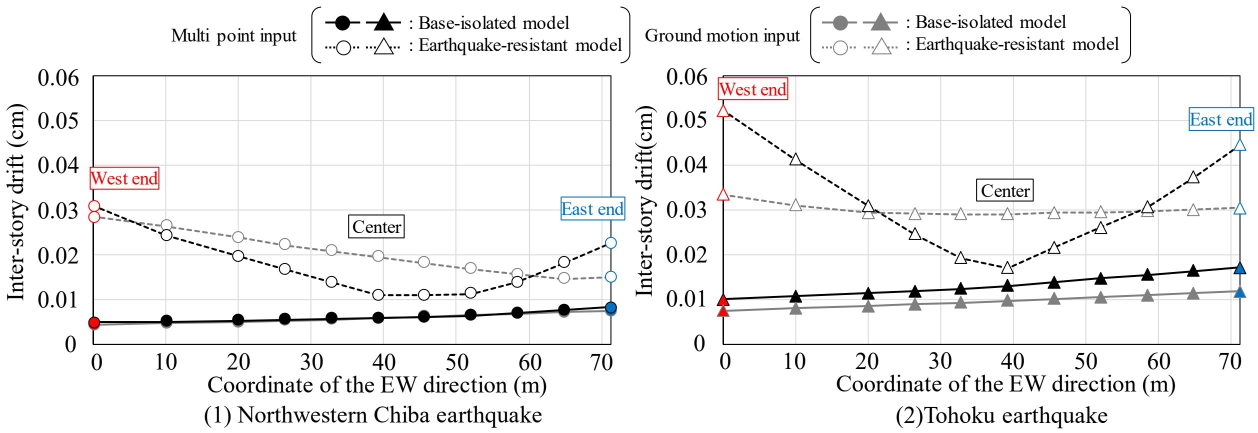

Fig. 13 Planar distribution of the inter-story drift of the sixth story

To evaluate the torsional response quantitatively, the following torsional response ratio β_{uN}[1) 8) 9)] was used:

$$\beta_{uN} = \Delta U_{uN} / U_{uC} = \frac{\max(|U_{uN}(t) - U_{uC}(t)|)}{\max(|U_{uC}(t)|)} \quad (2)$$

The relative displacement at the center of each floor, with respect to the center of the foundation, is defined as a reference displacement U_{uC}, and the ratio of the relative displacement to the incremental displacement ΔU_{uN} at each point on the same floor is evaluated as the torsional response ratio β_{uN}. Fig. 14 traces the torsional response ratios, obtained from the simulation results, in the NS direction at the west and east ends for both earthquakes. In both earthquakes, the base-isolated model has a much lower torsional response ratio than that of the earthquake-resistant model, indicating that the seismic isolation device has a great effect on reducing the torsional response of the upper structure. Tobita et al.[1)] calculated the torsional response ratio from the observation records of the foundation and 1F and revealed that the reduction of torsional motion in 1F became more pronounced as the maximum acceleration increased. During the Tohoku earthquake, in which the largest amplitude was recorded, the torsional response ratio in the base-isolated model is smaller than that observed in the Northwestern Chiba earthquake.

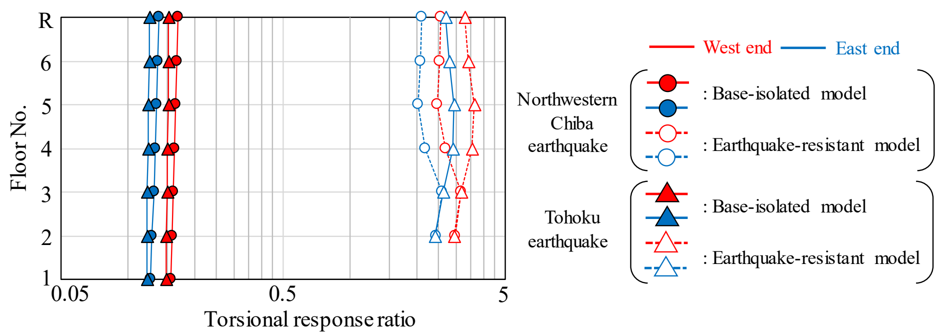

Fig. 14 The ratios of displacement due to torsional response of each point to displacement of the center of the building

5.3 Responses of the earthquake-resistant model

The Fourier amplitude spectra in the NS direction of the earthquake-resistant model at RF (west end, center, and east end) are traced in Fig. 15, and the first translational natural mode (NS direction) and the first torsional natural mode of the earthquake-resistant model are traced in Fig. 16. In the west end and the center of the earthquake-resistant model, the first natural frequency in the NS direction near 5.5 Hz (0.18 s) is predominant for both earthquakes. Another peak can also be seen around 4.5 Hz (0.22 s). From this, it can be considered that the torsional component greatly appears in the RF response in addition to the translational response.

As the cause of the increase in the maximum response at the west end in the earthquake-resistant model, the following can be presumed from the other analysis:

1. The first translational natural mode (NS direction) with a large deformation on the west side.
2. The first translational natural period in the NS direction (0.18 s) is close to the predominant period (0.14 s) obtained from the quarter wavelength rule at the west end of the ground. As seen in Fig. 3, the west end is actually predominant in this period.
3. The torsional mode is also excited in the building response because the first torsional natural period is 0.22 s and the input ground motion includes the torsional component.

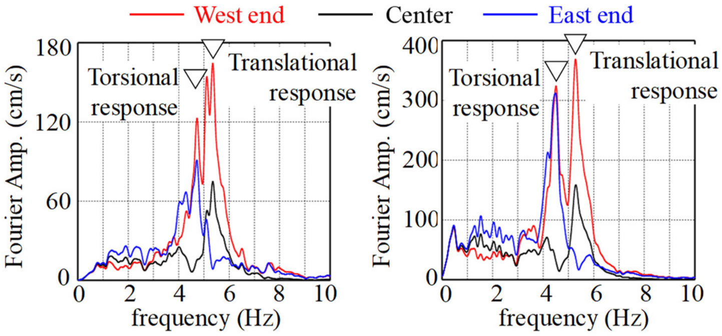

(a) Northwestern Chiba earthquake (b)Tohoku earthquake

Fig. 15 Fourier amplitude spectra at RF (NS direction)

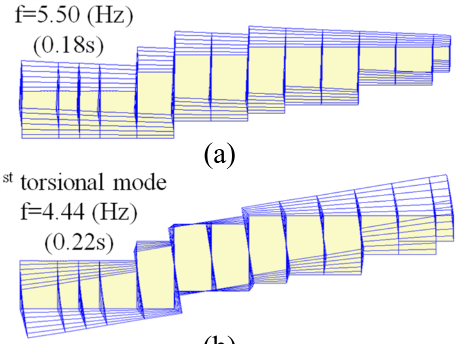

Fig. 16 Mode shapes of the earthquake-resistant model for (a) translational mode in short axis and (b) torsional mode

6. Conclusion

An observation records analysis and seismic response analysis using a 3D moment-resisting frame model and a 2D-FEM model for the subsurface structure were performed on the basis of the strong motion observation records at the base-isolated building constructed on soil with inclined bedrock. In addition, focusing on torsional response, we compared the responses of the base-isolated model and the earthquake-resistant model. The findings are summarized as follows.

① The predominant frequency of the observation records at the foundation indicates a difference due to the variance in layer thickness. In the west end, where the bedrock depth is shallow, the nearer the epicenter distance is, the higher the predominant frequency. At the east end, where the bedrock depth is deep, there is not much difference in the predominant frequency, depending on the epicentral distance, and it is dominated by the predominant frequency at the east end of the ground.

② According to the results of the seismic response analysis that used a base-isolated model and an earthquake-resistant model, the response of the upper structure was significantly reduced in the base-isolated model when compared to that in the earthquake-resistant model. Moreover, the reduction effect became more remarkable as the maximum amplitude of the input ground motion became larger. The maximum acceleration in the base-isolated model was larger from the 1F to the RF from the east end; this was consistent with the trend observed in the observation records on the 1F.

③ In the base-isolated model, the torsional response ratio was lower than that in the earthquake-resistant model; therefore, it can be said that seismic isolation devices are greatly effective in reducing the torsional response of upper structures. In addition, the greater the maximum amplitude of the input seismic motion, the more remarkable the reduction effect; this is consistent with the trend observed in the first-floor observation records of the entire upper structure.

Acknowledgments

We greatly appreciate the cooperation of the residents of the residential buildings during the microtremor measurements. Some figures were created using the Generic Mapping Tool (GMT).

References

[1] Y. Tobita, M. Nagano, H. Kitamura, T. Sato, K. Suzuki, Y. Matsuda, T. Yamauchi (2017): Study on torsional response pf seismically isolated building on soil with inclined bedrock using strong motion records. *AIJ J. Technol. Des.* Vol.23, No.54, 409-414.

[2] T. Watanabe, M. Iiba, K. Kato, N. Koshika (2011): A fundamental study on effects of inclined engineering bedrock on amplification characteristics in surface layer. *AIJ J. Technol. Des.* Vol.17, No.36, 455-459.

[3] N. Miyahara, M. Nagano, H. Kitamura, T. Sato, K. Suzuki, Y. Tobita (2016): Seismic response characteristics of seismically isolated building on inclined bedrock subsurface structure based on recorded motions during the 2011 Tohoku earthquake. Part 1 A study on the observed earthquake motion. *Summaries of technical papers of annual meeting, Architectural Institute of Japan,* 587-589.

[4] T. Morii, S. Takeuchi, K. Yoshida, M. Saruta, K. Adachi (2015): Effect of equivalent stiffness of seismic isolation device on environmental vibration assessment. *AIJ J. Technol. Des.* Vol.21, No.49, 1101-1105.

[5] Y. Tobita, M. Nagano, H. Kitamura, T. Yamauchi (2019): Seismic Response Analysis of Seismically Isolated Building Constructed on Soil with Inclined Bedrock Based on Strong Motion Records and Evaluation of Pile Stresses *J. Struct Constr. Eng., AIJ.* Vol.84, No.756, 149-159.

[6] Y. Tobita, R. Nishiura, H. Uebayashi, K. Suzuki, M. Nagano (2018): Dynamic Characteristics of Seismically Isolated Building on Soil with Inclined Bedrock using Microtremor Measurement Part1 Outline of Measurement and Results. *Summaries of technical papers of annual meeting, Architectural Institute of Japan,* 181-182.

[7] R. Nishiura, Y. Tobita, H. Uebayashi, K. Suzuki, M. Nagano (2018): Dynamic Characteristics of Seismically Isolated Building on Soil with Inclined Bedrock using Microtremor Measurement Part 2 Vibration Mode in the Predominant Frequency. *Summaries of technical papers of annual meeting, Architectural Institute of Japan,* 181-182.

[8] Y. Yamazaki (1986): Lateral Torsional Response of Buildings During Earthquakes *J. Struct Constr. Eng., AIJ.* No.369, 31-41.

[9] K. Suzuki, H. Sakata, Y. Yamazaki (2015): Experimental Study on Two Story Timber House with 3D Eccentricity *J. Struct Constr. Eng., AIJ.* Vol.80, No.709, 457-159.

[10] Wessel, P., Smith, W. H. F., Scharroo, R., Luis, J. F. and Wobbe, F. (2013). Generic Mapping Tools: Improved version released, EOS Trans. AGU, 94, 409-410.

